

Electroluminescence and electric current response spectroscopy applied to the characterization of polymer light-emitting electrochemical cells

Giovani Gozzi, Roberto Mendonça Faria, and Lucas Fugikawa Santos

Citation: *Appl. Phys. Lett.* **101**, 113305 (2012); doi: 10.1063/1.4752438

View online: <http://dx.doi.org/10.1063/1.4752438>

View Table of Contents: <http://apl.aip.org/resource/1/APPLAB/v101/i11>

Published by the AIP Publishing LLC.

Additional information on *Appl. Phys. Lett.*

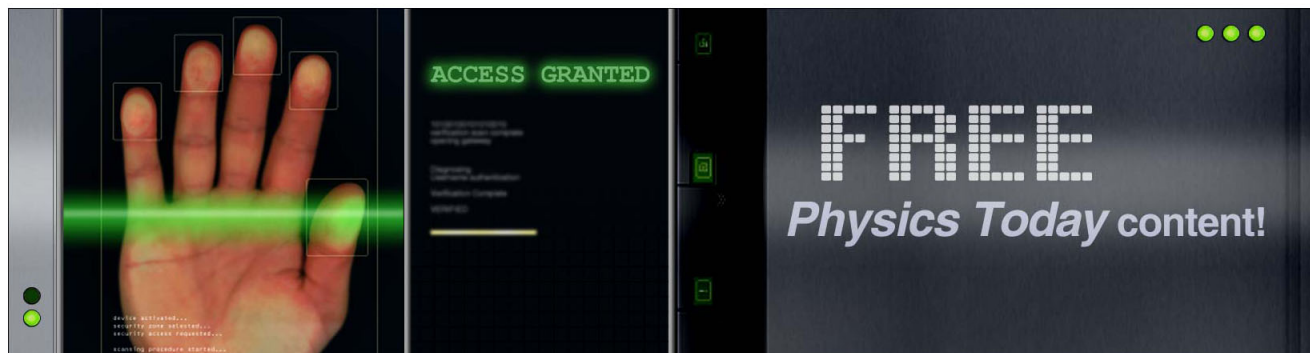
Journal Homepage: <http://apl.aip.org/>

Journal Information: http://apl.aip.org/about/about_the_journal

Top downloads: http://apl.aip.org/features/most_downloaded

Information for Authors: <http://apl.aip.org/authors>

ADVERTISEMENT



Electroluminescence and electric current response spectroscopy applied to the characterization of polymer light-emitting electrochemical cells

Giovani Gozzi,¹ Roberto Mendonça Faria,¹ and Lucas Fugikawa Santos^{2,a)}

¹Instituto de Física de São Carlos, Universidade de São Paulo, C.P. 369, 13560-250 São Carlos, SP, Brazil

²Departamento de Física, Campus de São José do Rio Preto, Universidade Estadual Paulista – UNESP, Rua Cristóvão Colombo, 2265, 15054-000 São José do Rio Preto, SP, Brazil

(Received 21 June 2012; accepted 28 August 2012; published online 13 September 2012)

Frequency-dependent electroluminescence and electric current response spectroscopy were applied to polymeric light-emitting electrochemical cells in order to obtain information about the operation mechanism regimes of such devices. Three clearly distinct frequency regimes could be identified: a dielectric regime at high frequencies; an ionic transport regime, characterized by ionic drift and electronic diffusion; and an electrolytic regime, characterized by electronic injection from the electrodes and electrochemical doping of the conjugated polymer. From the analysis of the results, it was possible to evaluate parameters like the diffusion speed of electronic charge carriers in the active layer and the voltage drop necessary for operation. © 2012 American Institute of Physics. [<http://dx.doi.org/10.1063/1.4752438>]

Light-emitting electrochemical cells (LECs) are optoelectronic devices which had been proposed¹ as an alternative to organic/polymeric light-emitting diodes (OLEDs/PLEDs) due to advantageous characteristics like low operation voltage, simple device structure, and bipolar electroluminescence behavior almost irrespective to the work-function of the metals used as electrodes. The device structure usually comprises a single active layer made of a blend of a polymer electrolyte and a organic semiconductor sandwiched between two electrodes which, differently from OLEDs/PLEDs, do not need matched work-functions to provide balanced charge-carrier injection enough to produce high electroluminescence at low voltages. The main explanation for this behavior is that, when the device is biased, ionic charges in the solid electrolyte are separated by the external electric field and drift towards each respective electrode, accumulating at the interfaces and facilitating the injection of electronic charge carriers into the organic semiconductor. The injected electronic charge carriers will then diffuse/drift and undergo recombination in the bulk, giving rise to the electroluminescence.

However, despite their advantages, LECs present also some drawbacks like slower electric and electroluminescence response, relative shorter lifetime, and lower stability, especially under excessive applied bias. Another key aspect that should be also mentioned is that there is still a lot of discussion about the main processes which govern the operation of LECs. The debate about the operating mechanisms of LECs can be summarized by considering the existence of two divergent models: an electrodynamic model (ED)² and an electrochemical doping model (ECD).^{1,3,4} The former predicts the formation of two electric double layers (EDL), which occurs due to the accumulation of uncompensated ions in the vicinity of both electrodes and screening the bulk material from the external applied field. As a consequence, the entire voltage drop is confined at the metal/active-layer interfaces, lowering

the energy barrier for injection of electronic charge carriers in the organic semiconductor and resulting in a diffusion-dominated electronic transport in the bulk.² On the other hand, in the ECD model, the ionic accumulation at the interfaces intermediates the electrochemical doping of the organic semiconductor, forming ohmic contacts and enhancing the further injection of electronic charge carriers in the bulk. The injection of electrons (holes) from the cathode (anode) promotes the electrochemical $n(p)$ -doping of the organic semiconductor in the bulk, giving rise to, in the steady-state, a n -doped semiconductor region and a p -doped region separated by an intrinsically undoped region (a p - i - n junction).⁴ In the undoped semiconductor region, the electric field is more intense than in the rest of the active layer and is where the recombination of electronic carriers mainly takes place.

Since the establishment of the controversy about the operating mechanism of LECs, several theoretical studies as well as experimental data have been presented as a conclusive proof to support one or the other model.^{5–10} Recently, a unifying model¹¹ has been proposed assuming that both ED and ECD models are simply operating regimes that differs by the injection rate (or the ability to form, or not, ohmic contacts), which will determine the dominant process in the device operation. In the same sense, previous works^{12,13} have shown clear evidences that the ED model is actually only a transitory process that precludes the electrochemical doping and the junction formation processes, which are the basis of the ECD model.

In this paper, we present an analysis of the current and the electroluminescence (EL) amplitude and phase as a function of the frequency of a modulating voltage to obtain information about the operating mechanisms of polymer LECs in a sandwich structure. From the obtained results, we conclude that depending on the applied voltage amplitude, and the frequency region that the device is operated, the ED or the ECD model can be used to explain the device characteristics.

Polymer light-emitting electrochemical cells (PLECs) were obtained by spin-coating the active layer comprising a blend of a conjugated polymer (poly(9,9-dioctylfluorene-2,7-

^{a)}Electronic address: lucas@sjrp.unesp.br. Tel.: +55 17 3221-2388. Fax: +55 17 3221-2247.

diyl)-co-(1,4-vinylene phenylene), known as ADS_GE) and a polymeric electrolyte (poly(ethylene oxide), PEO, mixed to lithium trifluoromethanesulfonate, $\text{CF}_3\text{SO}_3\text{Li}$) onto ITO covered glass substrates. The blend solutions were prepared in such a way that the final weight ratio of ADS_GE:-PEO: $\text{CF}_3\text{SO}_3\text{Li}$ was 10:10:1. The obtained blend films were about 300 nm thick, and aluminum top-electrodes (150 nm thick and 10 mm² in area) were thermally evaporated in a high-vacuum deposition system inside an inert gas glove-box. All the device preparation steps (described in detail in Ref. 14) and characterization experiments were carried out in inert atmosphere conditions, avoiding any exposure to oxygen and moisture.

Two different experimental setups were used to characterize the LEC devices: (i) electrical impedance/admittance measurements using a Solartron Instruments gain/phase frequency response analyzer (FRA) model 1260 A and (ii) EL frequency response measurements using a function/signal synthesizer (Hewlett-Packard HP3325 model) to drive the device current and a calibrated silicon fast photodiode coupled to the transimpedance amplifier input of a Keithley 610 C electrometer in which analog output was connected to the input of a 500 MHz bandwidth oscilloscope (Agilent HP54610B model) to register the EL light output and its respective phase-shift to the applied voltage and drive current. All the measurements were carried out with the ITO electrode biased by a sinusoidal signal varying from 0 V (the lowest value in a complete cycle) up to a definite positive value.

Figure 1 shows the applied voltage, device current, and EL output signal as a function of the time for different modulation frequencies from 0.5 Hz up to 200 Hz. The applied peak-to-peak voltage is 8 V. From these results, one can see that, in the considered frequency range, the current presented a practically in-phase response relative to the excitation voltage, which can be clearly noticed by the coincidence in the current and voltage valleys. Such a behavior is characteristic of systems where the conductive nature overcomes the capacitive nature. At the lowest observed frequency (0.5 Hz,

Fig. 1(d)), a slight deformation of the current from a sinusoidal signal occurs, due, probably, to the time needed to form the steady state electrochemical junction. At the highest frequency shown (200 Hz, Fig. 1(a)), the EL output is practically constant in time, showing that charge recombination still takes place when the applied voltage is null and the current drops to its lowest value. For lower frequencies, EL output amplitude modulation becomes more evident and, at sufficiently low frequencies (Figs. 1(c) and 1(d)), it is possible to distinguish when the device is on or off. It is important to notice also that the EL amplitude (or rms value) increases considerably when the modulation frequency decreases. In these cases, it is possible to define the phase-shift between the EL and the device current from the time delay between the EL peak and the current peak.

In the same sense, the EL efficacy (which is proportional to the EL efficiency) was defined as the ratio between the maximum luminance intensity and the maximum value of the current in a cycle. The modulus of the EL efficacy ($|L^*|$) and the phase-shift relative to the device current (ϕ) are shown as a function of the voltage modulation frequency in Fig. 2. It is important to notice that, for frequencies higher than 100 Hz, the phase-shift could not be practically defined anymore, since the EL output becomes constant in time.

In Fig. 2, one can identify three different frequency regions where the modulus of the EL efficacy presents distinct behaviors: (i) at frequencies below 5 Hz, where the phase angle is non-null and practically constant (about $-\pi/8$ rad) and the modulus of L^* has an empirical $f^{-0.5}$ dependence with the frequency; (ii) between 5 Hz and 50 Hz, where the modulus is practically frequency independent and the angle phase presents a linear dependence with the frequency; and (iii) at frequencies above 50 Hz, where the EL efficacy modulus starts to decrease with frequency, following approximately an empirical $f^{-0.22}$ dependence and the EL stops to follow the voltage modulation.

In regime (i), one can observe that the EL efficacy achieves relatively high values in the low-frequency region

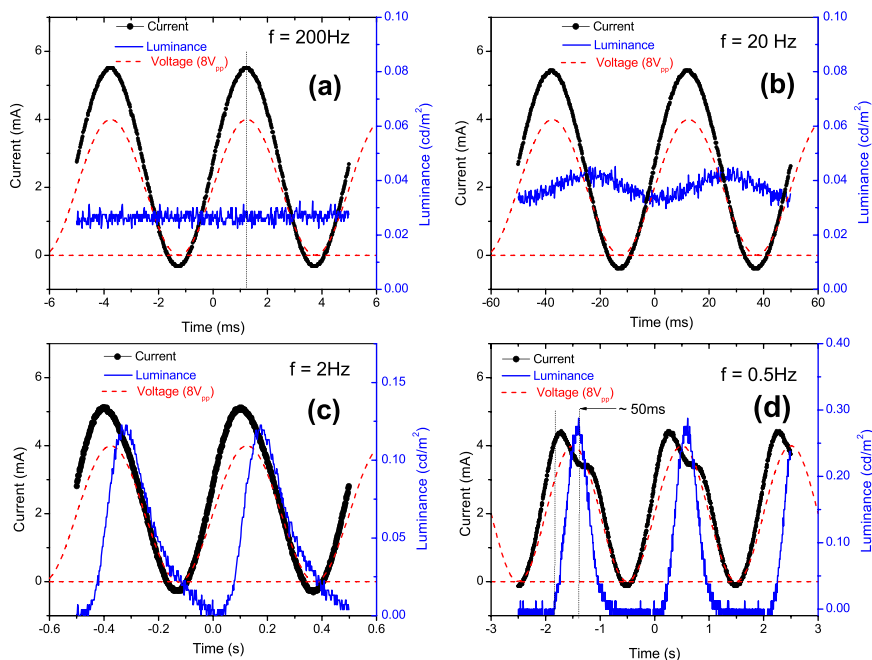


FIG. 1. Device voltage, current, and EL output as a function of the time for different modulation frequencies. Modulation voltage amplitude: 8Vpp. (a) 200 Hz; (b) 20 Hz; (c) 2 Hz; (d) 0.5 Hz.

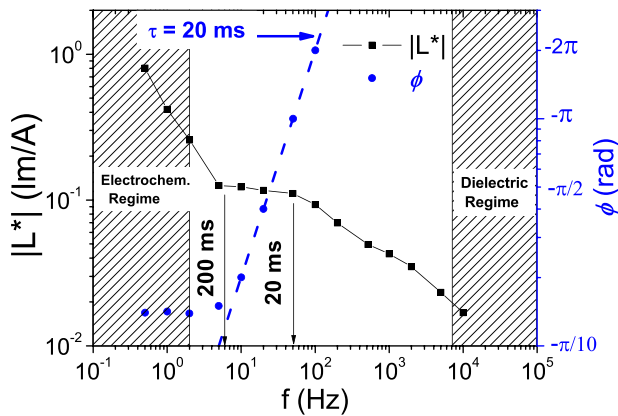


FIG. 2. Frequency dependence of the amplitude and phase shift relative to the modulation voltage of the device luminous efficacy.

(below 5 Hz, which means a cycle period higher than 200 ms). In a recent report,¹⁵ we have shown results supporting that the steady-state of devices with similar characteristics than the ones presented here is reached about 300 ms after the application of a voltage step. The present results corroborate that the electrochemical doping (oxidation close to the anode and reduction close to the cathode) of the conjugated polymer and the subsequent formation of a *p-i-n* junction⁵ need a time of about few hundred milliseconds to take place. Moreover, in this regime, since the phase-shift is constant (about -22.5°), the EL reaches its maximum value always at the same voltage (or current) value (here, at about 5.7 V). From Fig. 1(d), it is possible to see that the maximum of the EL has an almost constant delay of 50 ms from the onset of the EL, which occurs at an approximate voltage of 4.0 V. This onset voltage is frequency independent in this regime and is in accordance to the expected onset voltage of about 3.5 V for this kind of device.¹⁵

For higher frequencies, in regime (ii), the EL efficacy is almost constant with the frequency and the EL phase-shift behavior changes dramatically, varying linearly with the frequency. This behavior can be explained if we consider that, for times shorter than 300 ms, the injection of electronic charges from the electrodes is lower than in the quasi-d.c. regime and the electrical response of the device is mainly dominated by interfacial accumulation of charges, giving rise to electric double layer formation close to each electrode.^{10,11} In this regime, the internal electric field in the bulk is negligible, due to screening from the accumulated ionic charges at the polymer/electrode interface. As a result, the transport of the injected electronic charges in the bulk is carried out by diffusion, which does not depend on the modulating frequency and on the external applied voltage. In this frequency region, the EL does not fall down to zero because of the independence of the diffusion process from the external voltage (Fig. 1(b)). However, the EL output still presents some modulation with the excitation signal because the injection of the electronic charges that undergo diffusion is a voltage-dependent process. Another interesting point is that the phase angle has a linear dependence with frequency, with an angular coefficient equal to 2×10^{-2} s, obtained from Fig. 2. This time can be associated to the time needed for the charge carriers to diffuse from the electrodes to the recombination region. Considering

that the recombination occurs about the center of the polymeric film, one can obtain a diffusion speed of 7.5×10^{-4} cm/s.

For even higher frequencies (above 100 Hz), the period of the modulating voltage becomes shorter than the diffusion time, eliminating the injection limitation for the electroluminescence and making the light output time-independent, as shown in Fig. 1(a). However, as the frequency increases, a greater number of cycles will be contained in a same time frame in such a way that the contribution of the injection to the total device current will decrease and, consequently, the EL efficacy will also decrease (Fig. 2).

To corroborate the previous analysis, electric impedance/admittance measurements in the frequency domain were performed using a gain/phase frequency response analyzer. Fig. 3 shows the modulus of the complex conductivity, the modulus of the complex dielectric function, and the phase-shift between the modulating voltage and the corresponding current, as a function of the frequency, for a device biased by a sinusoidal signal with the amplitude varying from 0 V up to +0.5 V, +1 V, and +3 V, respective to the ITO electrode.

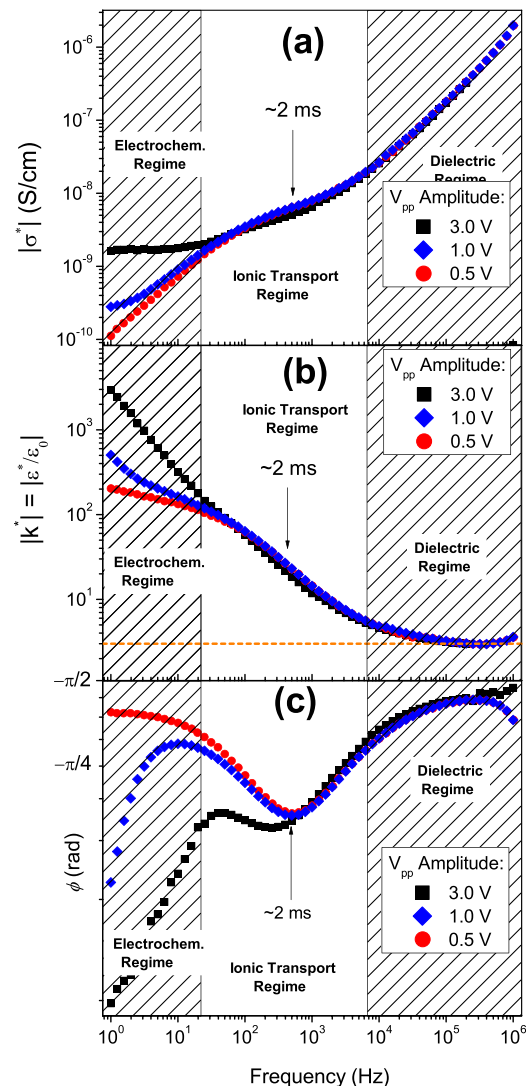


FIG. 3. Voltage amplitude dependence of different complex frequency response electric functions. (a) Modulus of the complex conductivity; (b) modulus of the complex dielectric function; (c) phase-shift of the electric current to the excitation voltage.

For low voltages ($V_{pp} = 0.5$ V), the phase-shift has values close to $-\pi/2$ for high frequencies ($>10^4$ Hz) and also for low frequencies (<20 Hz). A $-\pi/2$ phase-shift can be interpreted as a capacitive system in which conduction is almost negligible. The modulus of the dielectric function, at frequencies above 10^4 Hz, is about 3, which is a reasonable value for polymeric dielectrics. This means that the ionic transport does not take place in the high frequency region and the device behaves like a dielectric capacitor. Moreover, in this frequency region, the electrical conductivity and the dielectric function do not show any dependence on the applied voltage, as expected for a purely capacitive system. Hence, we say that, in this frequency region, the PLEC is operating in its “dielectric regime.”

For frequencies between 20 Hz and 10 kHz, the modulus of the phase-shift clearly diverges from $\pi/2$, presenting a minimum around 500 Hz (for $V_{pp} = 0.5$ V, Fig. 3), which indicates an increase of the conductive contribution to the total electric current. Moreover, an increase of almost two orders of magnitude in the dielectric function is observed in this frequency range, which means that the increase in the conductive contribution to the current is probably due to the establishment of the ionic transport in the polymeric electrolyte. Another evidence for this effect is due to ionic transport at frequencies below 10 Hz, the phase-shift tends back to $-\pi/2$, and the dielectric function becomes again almost constant; what is consistent if we consider that the electrodes are blocking for ions. Therefore, the formation of the electric double layer takes place mainly in this frequency range, which defines the “ionic transport regime” illustrated in Fig. 3. When the amplitude of the voltage is increased ($1V_{pp}$ and $3V_{pp}$), the modulus of the phase-shift decreases very fast in the low frequency region, evidencing that another conductive contribution to the total current takes place. This conductive contribution comes from the injection of electronic charge carriers from the electrodes, which is facilitated by the accumulation of the ionic charges at the polymer/metal interfaces. As a result of the higher electronic carrier injection, the modulus of the complex conductivity increases, assuming, for $V_{pp} = 3$ V, an almost constant value at low frequencies (Fig. 3(a)), which is characteristic of a conductive system in the d.c. regime. For $V_{pp} = 0.5$ V, the slope of the conductivity at frequencies below 20 Hz recovers the same value than for frequencies above 10 kHz, showing that after the ionic transport saturates, due to the ion-blocking electrodes, the device behaves again almost like a capacitor, with low d.c. conductivity.

A further increase in the dielectric constant is observed in the low frequency region and at higher applied voltage amplitude (Fig. 3(b)). This effect is related to the higher electronic charge-carrier injection and the subsequent electrochemical doping of the conjugated polymer. With the formation of a steady-state $p-i-n$ junction, the complex conductivity becomes practically constant with the frequency (equal to the d.c. conductivity value) and, since $|\sigma^*| = \omega^2 |\epsilon^*|$, the complex dielectric function will show a fast increase as the frequency decreases.

Figure 4 shows the dependence of the d.c. conductivity on the amplitude of the applied voltage, obtained from the low-frequency value of the modulus of the complex conductivity (Fig. 3(a)). For $V_{pp} = 0.5$ V, the d.c. conductivity could

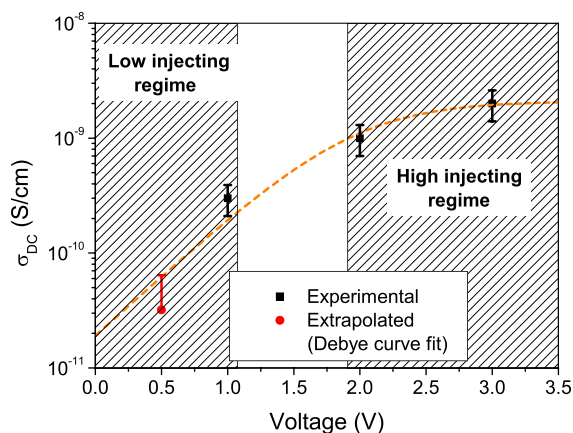


FIG. 4. Behavior of the d.c. conductivity on the amplitude of the applied voltage. The data were obtained from the low-frequency value of the real part of the complex conductivity (Fig. 3(a)). The red circle indicates the value for 0.5 V which had to be extrapolated using a Debye fitting.

not be obtained directly from the graph and was determined by extrapolation using a single Debye relaxation fitting. An increase of about two orders of magnitude is observed in the voltage range from 0 V to 3 V, due to the increase in the charge carrier injection and also to the electrochemical doping of the conjugated polymer. For voltages higher than 3 V, the d.c. conductivity shows a trend to become constant, which is consistent with the picture that the electrochemical doping process is accomplished and that the d.c. current assumes a quasi-linear dependence on the applied voltage, as reported previously.^{12,15,16}

The proposed experimental methods and analysis introduced here enabled us to identify the different operation regimes of light-emitting electrochemical cells and their relationships with the modulating frequency and the amplitude of the applied voltage. At high frequencies (above 10 kHz), a dielectric regime was observed, where the electrical characteristics of the devices are similar to a dielectric capacitor, with low ionic and electronic conductivity, independence on the applied voltage, and very low EL efficiency. At intermediate frequencies (between 20 Hz and 10 kHz), a regime characterized by the drift of ions in the polymer electrolyte and diffusion of electronic charge-carriers in the conjugated polymer was observed, with relative increase in the EL efficiency and huge increase of the modulus of the complex dielectric constant. At frequencies below 20 Hz and for voltages higher than the device onset voltage (about 3.5 V), a regime characterized by higher values of EL efficiency and of d.c. conductivity is achieved, as a consequence of the establishment of an electrochemical $p-i-n$ junction. Therefore, the obtained results can be used to corroborate that the electric double layer formation and electronic diffusion processes are merely transitory and preliminary conditions necessary for the electrochemical doping of the conjugated polymer and subsequent formation of the $p-i-n$ junction, as predicted by the ECD model,^{12,13} since only after the establishment of the junction, the LECs present high electroluminescence efficiency values.

The authors acknowledge the financial support from Brazilian agencies FAPESP, CNPq, and National Institute of

Organic Electronics (INEO). L.F.S. thanks the fellowships granted by CNPq and CAPES.

- ¹Q. Pei, G. Yu, C. Zhang, Y. Yang, and A. J. Heeger, *Science* **269**, 1086 (1995).
- ²J. C. DeMello, N. Tessler, S. C. Graham, and R. H. Friend, *Phys. Rev. B* **57**, 12951 (1998).
- ³D. L. Smith, *J. Appl. Phys.* **81**, 2869 (1997).
- ⁴J. A. Manzanares, H. Reiss, and A. J. Heeger, *J. Phys. Chem. B* **102**, 4327 (1998).
- ⁵J. D. Slinker, J. A. DeFranco, M. J. Jaquith, W. R. Silveira, Y. W. Zhong, J. M. Moran-Mirabal, H. G. Craighead, H. D. Abruña, J. A. Marohn, and G. G. Malliaras, *Nature Mater.* **6**, 894 (2007).
- ⁶J. H. Shin, N. D. Robinson, S. Xiao, and L. Edman, *Adv. Funct. Mater.* **17**, 1807 (2007).
- ⁷D. Hohertz and J. Gao, *Adv. Mater.* **20**, 3298 (2008).
- ⁸Y. Lei, F. Teng, Y. Hou, Z. Lou, and Y. Wang, *Appl. Phys. Lett.* **95**, 101105 (2009).
- ⁹M. Lenes, G. Garcia-Belmonte, D. Tordera, A. Pertegás, J. Bisquert, and H. J. Bolink, *Adv. Funct. Mater.* **21**, 1581 (2011).
- ¹⁰S. van Reenen, P. Matyba, A. Dzwilewski, R. A. J. Janssen, L. Edman, and M. Kemerink, *Adv. Funct. Mater.* **21**, 1795 (2011).
- ¹¹S. van Reenen, P. Matyba, A. Dzwilewski, R. A. J. Janssen, L. Edman, and M. Kemerink, *J. Am. Chem. Soc.* **132**, 13776 (2010).
- ¹²Q. Pei, Y. Yang, G. Yu, C. Zhang, and A. J. Heeger, *J. Am. Chem. Soc.* **118**, 3922 (1996).
- ¹³Q. Pei and A. J. Heeger, *Nature Mater.* **7**, 167, 168 (2008).
- ¹⁴See supplementary material at <http://dx.doi.org/10.1063/1.4752438> for details on the samples preparation procedure.
- ¹⁵G. Gozzi, L. F. Santos, and R. M. Faria, "Transient and d.c. analysis of the operation mechanism of light-emitting electrochemical cells," *Europhys. Lett.* (submitted).
- ¹⁶L. F. Santos, L. M. Carvalho, F. E. G. Guimarães, and R. M. Faria, *Synth. Met.* **121**, 1697 (2001).